

CREATION OF HETEROJUNCTIONS AND PERIODICAL STRUCTURES IN SOLID SOLUTIONS BY LASER ANNEALING

M.M.Pociask, E.M.Sheregii, M.Kuźma

Institute of Physics, Pedagogical University in Rzeszów,
Rejtana 16a Str., 35-310 Rzeszów, Poland,
e-mail: pociask@atena.univ.rzeszow.pl

Thermodiffusion model of laser annealing and decomposition of the material is presented. It has been shown that phonon flux plays a significant role in this process. The magnitude of the phonon flux is closely related to the area of the material, where the temperature gradient has a significant value, as a result of which Hg atoms are gathered in a place corresponding to the maximum value of the temperature gradient. It has been shown that the processes of atoms diffusion at laser annealing of HgCdTe (MCT) can cause the specific conditions of decomposition of the solid solution. The idea of the possible formation of *p-n* heterojunction, which was shown by computer modelling of mass transportation processes under laser treatment of the MCT was experimentally realized. MCT samples were irradiated without melting with an YAG neodymium laser. The presence of a heterojunction not far below the surface has been verified by photovoltaic measurements and X-ray microanalysis as well as by current-voltage characteristics.

Mercury cadmium telluride solid solution is still one of the most important material for infrared devices. However, that kind of semiconductors has a serious fault: the weak mercury bond in crystal net. The velocity of mercury diffusion coefficient is significant even at room temperature, therefore physical properties of mercury cadmium telluride depend on diffusion processes of mercury. After obtaining HgCdTe thermal heating is used for improvement of its properties.

On the other side, this peculiarity - the weak HgTe bond - has an another aspect: the possibility to modify the properties of that material by external influences, for example, by laser irradiation.

The results of recent investigations for MCT semiconductors group after laser annealing are contradictory. Some of them give the evidence for the influx of Hg atoms to the irradiated material surface [1–3] and influx of Te atoms to this surface [4], others indicate the outflux of mercury atoms from annealed surface [5,6]. Ref. [7] presents ambiguous data on laser annealing of HgCdTe without melting.

In this paper it is shown that the diffusion processes of atoms at laser annealing of $\text{Hg}_{1-x}\text{Cd}_x\text{Te}$ can cause the specific conditions of decomposition of solid solution which determine its inner periodic structure.

The possibility of obtaining sharp *p-n* junctions in $\text{Hg}_{1-x}\text{Cd}_x\text{Te}$ by laser treatment has been reported earlier [8,9]. The authors of Ref. [8,9] restricted their analysis to the quantity aspect of the dynamic of one of the ingredients (mercury). But there is a lack of diffusion model describing changes in physical properties of mercury cadmium telluride in the presence of high-power laser beam.

The purpose of this paper is to describe the thermodiffusion model of mass transport mechanism at laser annealing condition and subsequent verification results of simulation of mercury diffusion processes by microanalyses of components of MCT specimens after annealing.

Thermodiffusion model

Diffusion processes are described by the standard diffusion equation. However, there is

a large increase in the diffusion parameters, such as diffusion coefficient, length of diffusion, etc. [10, 11] in the case of laser annealing. This is caused mainly by the following factors: large temperature gradients (for time pulse length equal to 250 μs they are even about 1000 K per centimetre), which produce the flux of phonons ("phonon wind") taking impurity atoms away, and the field of thermoelastic deformations [12, 13].

These factors are taken into account in the diffusion equation by the additional atom flux arising from the action of the phonon wind at the laser annealing [14, 15]:

$$\frac{\partial N}{\partial t} = \nabla \left(D \nabla N - \frac{D}{k_B T} \left\langle \frac{\tau_f}{\tau_{fi}} \right\rangle \frac{C_V}{3N_i} \nabla T \right), \quad (1)$$

where $D = D_0 \exp(-E_a / k_B T)$ is mercury diffusion coefficient, E_a – the activation energy of vacancy creation, C_V – specific heat, N – the impurity concentration, ∇T – the temperature gradient.

One can notice from Eq. (1) that the direction of diffusion of atoms or defects caused by phonon wind depends on the sign of the second term in the right side of (1) and therefore de-

pends on the sign of the derivative of the temperature gradient. This means the inversion of sign in the case, when an extremum of the temperature gradient exists, provides an influx of atoms or defects from two sides to the point of the temperature gradient extremum. At this point atoms are gathering.

To solve the diffusion equation the information about temperature and temperature gradient fields is necessary. The required information can be obtained by solving the thermoconductivity equation. The standard thermoconductivity equation must be complemented with the term describing the laser energy:

$$\frac{\partial T}{\partial t} = a \Delta T + \frac{W e^{-\alpha x}}{\lambda}, \quad (2)$$

where a is temperature conductivity coefficient, α – laser absorption coefficient, x is the analysed depth of the sample, λ – thermoconductivity, W – the power of the laser beam absorbed by a volume unit of the sample.

One of the methods of solving this differential equation is a finite-difference method [16]. For this purpose both these equations were used in the subtraction form:

$$\frac{N_i^{k+1} - N_i^k}{\tau} = D_0 e^{-E_a / k_B T_i^{k+1}} \left[\frac{N_{i-1}^{k+1} - 2N_i^{k+1} + N_{i+1}^{k+1}}{h^2} - \frac{C_V}{3k_B T_i^{k+1}} \frac{T_{i-1}^{k+1} - 2T_i^{k+1} + T_{i+1}^{k+1}}{h^2} \right], \quad (1a)$$

$$-\frac{a\tau}{h^2} T_{i-1}^{k+1} + \left(1 + \frac{2a\tau}{h^2} \right) T_i^{k+1} - \frac{a\tau}{h^2} T_{i+1}^{k+1} = T_i^k + \frac{aW\tau}{\lambda} e^{-\alpha h(i-1)}, \quad (2a)$$

where k is a number of time layer, i is a number of spatial layer ($i = 1, 2, 3, \dots, 30$), h is a spatial step ($h = d/30$), $d = 30 \mu m$, and τ is a time step (the details of the calculation procedure are presented in [15]).

For this method the stability condition is the following: $\tau \leq \frac{1}{2} \frac{h^2}{\kappa}$, (κ is equal to D for thermodiffusion equation or κ is equal to a for thermoconductivity equation). This means that the space step must be much greater than diffu-

sion length in the case of diffusion equation, and in the case of thermodiffusion equation - than the heat transport during the time step.

Our considerations were restricted to the one-dimensional case, because the condition for one-dimensionality is fulfilled here: the diameter of the homogenous laser beam is much greater than the thickness of the sample. Equation (1a) enables us to interpret the nature of the local concentration of impurities caused by phonon wind (the last term in (1a) after laser

annealing. It can be seen from equation (1a) that the sign of the second term on the right side of the equation depends on the sign of the curvature of the temperature distribution. The set of 30 linear equations for 30 spatial layers (we assumed this number of layers) should be solved for each time step.

The calculations were performed for specimen of HgCdTe ($x=0.2$) for first 30 layers (the width of each layer is $1\mu\text{m}$). YAG: Nd³⁺ laser ($\lambda=1.06\text{ }\mu\text{m}$, pulse time $t=250\mu\text{s}$) was chosen.

In MCT semiconductors the prominent role is played by intrinsic defects such as vacancies of mercury atoms which are acceptors, and interstitial mercury atoms (IMA) which are donors. At high temperature the main model of diffusion of IMA in HgCdTe is a vacancy mechanism, which allows the chemical diffusion of mercury. This diffusion process of IMA determines the concentration of both donors and acceptors and brings about a change in chemical composition of the material [17]. For this reason the initial concentration of IMAs was accepted as $N_i^0 = 1 \cdot 10^{21} \text{ m}^{-3}$. An increase in the concentration of defects is included into the thermal dependence of the diffusion coefficient $D(T) = D_0 \exp(-E_a/k_B T)$. The diffusion parameters are the following: $D_0 = 6 \cdot 10^{-6} \text{ m}^2 \text{ s}^{-1}$, $E_a = 0.96 \text{ eV}$ [18].

Thermoconductivity equation was solved under the following boundary and initial conditions: the initial temperature of the semiconductor was equal to room temperature; a linear gradient of temperature on the other side of the sample, where the layer is contact with the substrate, was assumed; the irradiated surface was assumed to be thermally isolated from the environment. In the boundary conditions for the diffusion equation the concentration of mercury in the air was taken as $N_0 = 0$. That determines the negative diffusion, i.e. mercury atoms are evaporated from the irradiated surface (the first layer). It was also assumed that

$$N_0^k = N_k^1 \operatorname{erf}\left(\frac{H}{2\sqrt{Dt}}\right),$$

$$N_{31}^k = N_{30}^k \operatorname{erfc}\left(\frac{h}{2\sqrt{Dt}}\right)$$

where $\operatorname{erfc}(y) = 1 - \operatorname{erf}(y)$ is the Gauss error function, N_{31} is the concentration of IMAs in the first layer in the sample, and N_{30} is the last layer in the annealed width of the sample.

The following parameters describing the thermal properties of the sample were used for the calculation: mass density $\rho = 7.63 \cdot 10^3 \text{ kg}\cdot\text{m}^{-3}$, $\lambda = 4.3 \text{ W}\cdot\text{m}^{-1}\cdot\text{K}^{-1}$, $\alpha = \lambda/\rho \cdot C_v$, $\alpha = 8.3 \cdot 10^{-6} \text{ m}^2 \cdot \text{s}^{-1}$, the melting temperature of $\text{Hg}_{0.8}\text{Cd}_{0.2}\text{Te}$ is $T_i = 1050 \text{ K}$, the laser beam power was fitted in order to keep the maximum temperature in the sample less than T_i [19].

Results of simulations and discussion

In our calculations the diffusion of interstitial mercury atoms was simulated.

The results of calculations of the time-spatial distribution of the temperature gradient and concentration of IMAs in HgCdTe for the laser pulse length $t=250\text{ }\mu\text{s}$ are presented in Fig. 1. More results of simulation for different parameters of laser annealing are presented in our previous paper [15]. As can be noticed from Fig.1a, the temperature gradient exists into the whole investigated depth of material and is equal to 10^3 K/cm . As one can see from Fig. 1b, laser treatment induces a non-homogenous distribution of IMAs and causes a sharp maximum in the IMA concentration with a value two times greater than the initial value, after laser treatment by three successive pulses. The maximum is at a depth of $1.2\mu\text{m}$ from the surface and this position correlates with the position of the extremum of ∇T (Fig.1a). Comparing these results with those in Fig.1c, where the concentration distribution was calculated without the last term in Eq. (1), we can state that this non-homogenous concentration is caused only by phonons.

Experimental results

With the aim of experimental verification of the computer simulated results, the distribution of Hg concentration in HgCdTe specimens subjected to laser treatment was investigated under the above mentioned conditions ($\lambda = 1.06 \mu\text{m}$, $t = 250 \mu\text{s}$, energy density of the beam $0.82 \text{ J}\cdot\text{cm}^{-2}$). Annealing was performed with three successive pulses. Before irradiation the samples were chemically etched. With the aim of obtaining sufficient resolution of the measurements a wedge with an angle of 2° , was made on the surface of the sample. The concentration distribution was determined by micro X-ray analysis using a XL30 Philips spectrometer by scanning an electron beam along the wedge surface. The distribution of Hg, Cd, Te concentrations before (dashed lines) and after (solid lines) annealing of *p*-type epitaxial layer (pEL2) group samples and *n*-type bulk (bN2) group samples is presented in Figs. 2a and 2b.

It can be seen from Figs. 2a and 2b that the non-monotonous concentration curves appeared after laser treatment without melting. It can be seen that the laser annealing has caused a decrease in the Hg concentration on the irradiated surface. The first maximum of the Hg concentration is at the depth of $1.5 \mu\text{m}$ from the irradiated surface. This position is in agreement with the maximum of the Hg concentration caused by the thermodiffusion effect discussed above. Nevertheless, the next maxima appear. The minima of the Cd concentrations correspond to the maxima of the Hg concentration. The tellurium concentration has also changed. In the case of bulk *n*-HgCdTe group of probes nB2 (Fig.2b) the distinct phase opposition for oscillations of Hg and Cd component concentrations has been observed, and phase shifting of both of these dependences can thus be stated. The new feature for the curves in Fig. 2b can be noticed: distances between adjacent maxima (minima) became larger with depth being increased. Oscillations are attenuated at a depth of $13\text{-}14 \mu\text{m}$. Similar depth profiles for other kinds of sample (low and high *p*-bulk) have been obtained.

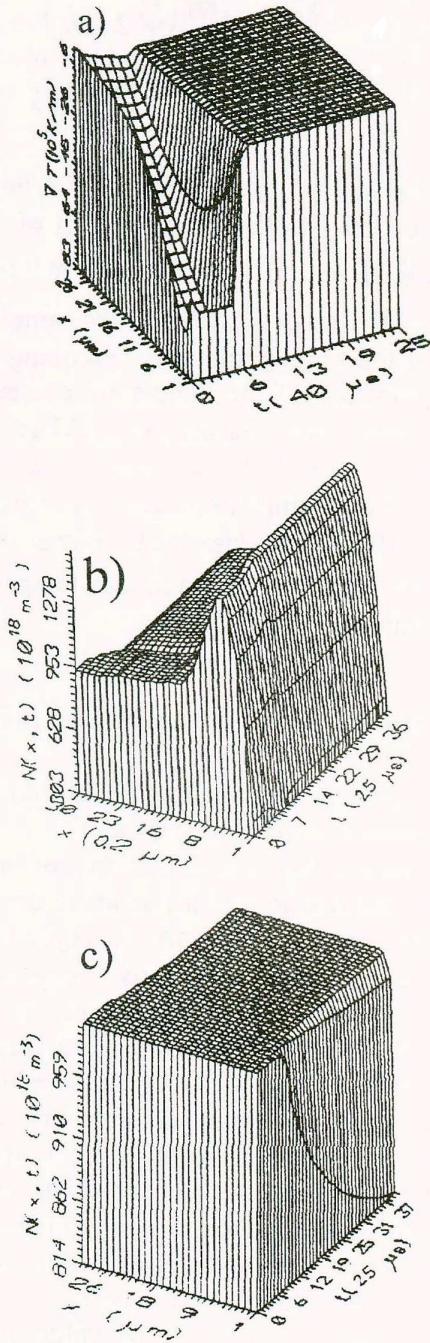


Fig.1.a) Time spatial distribution of the temperature gradient $\nabla T(x,t)$ with pulse after irradiation of pulse length of $t=250 \mu\text{s}$ and absorbed power density $W=3.08 \cdot 10^{13} \text{ W}\cdot\text{m}^{-3}$ and absorption coefficient $\alpha=1 \cdot 10^6 \text{ m}^{-1}$.

b) Time spatial distribution of the mercury concentration $N(x,t)$ after irradiation by three successive pulses with length $t=250 \mu\text{s}$ (parameters of annealing as in (a)).

c) Time spatial distribution of the mercury concentration $N(x,t)$ without the action of the phonon wind (parameters of annealing as in (a)).

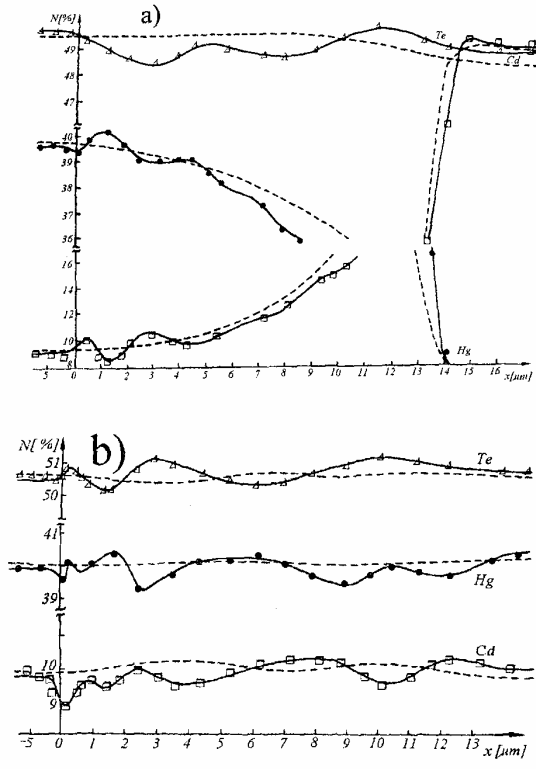


Fig.2. Depth profiles of laser irradiated (solid curves) and nontreated (dashed curves) areas for: a) epitaxial layers $p\text{Hg}_{0.8}\text{Cd}_{0.2}\text{Te}$ (pEL2), b) bulk $n\text{Hg}_{0.8}\text{Cd}_{0.2}\text{Te}$ (nB2). (Δ)Te, (\bullet)Hg, (\square)Cd.

The possibility of interpreting the experimentally obtained oscillations of concentration can be explained with the help of Khachaturian [21] and other [22, 23] thermodynamical models of the two-component solid solution.

Following this thermodynamical model we can say that the amplitude changes of the concentration oscillations with a depth x can be related to the different thermal history in various points of the sample at laser annealing.

At the laser annealing great temperature gradients arise, which can cause thermodiffusion of the Hg atoms. This leads to a local maximum of Hg concentration. Therefore, the sample becomes divided into two parts with unbalanced thermodynamical equilibrium. This results in the metastable state of the two-component solid solution, which undergoes decomposition into mixing of two phases with different concentrations [20]. This decomposition leads to the regular oscillations of composition.

Theoretical (Fig. 1b) and experimental (Fig. 2a, 2b) distributions are in a good agreement.

The mercury segregation at the depth of about $1.5 \mu\text{m}$ and Hg lower concentration near the surface can cause a decrease in the energy gap and vice versa. The mechanism of formation of the heterojunction in this case is following: the annealing of the surface layer causes a significant loss of Hg atoms, thus forming a great number of Hg vacancies. This leads to an inversion of the type of conductivity of the surface layer, i.e. a p - n junction is formed. The model of the p - n heterojunction is shown in Fig.4b.

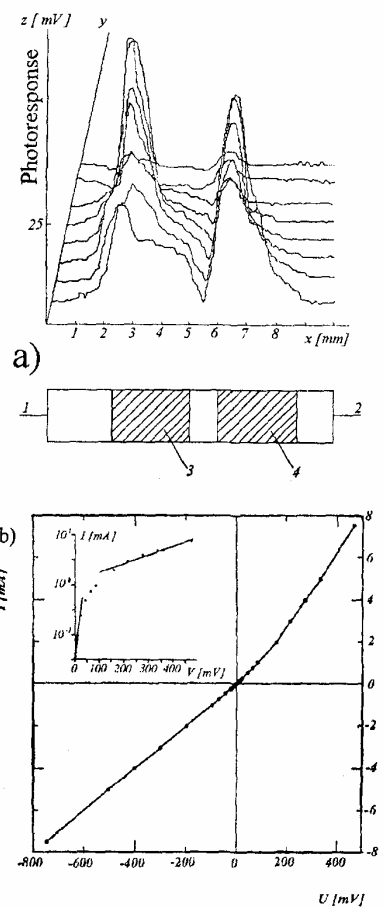


Fig.3. a) Photoresponse obtained from the contacts (1,2) in the photovoltaic regime during the process of scanning by the CO laser ($\lambda_{\text{Co}}=5.33 \mu\text{m}$, $E=0.7 \text{ J cm}^{-2}$) probe in steps of 0.1mm over the $n\text{Hg}_{0.8}\text{Cd}_{0.2}\text{Te}$ (nB3) surface containing the annealed areas (3,4).

b) Current-voltage characteristic for the sample $n\text{Hg}_{0.8}\text{Cd}_{0.2}\text{Te}$ (nB4) after annealing with neodymium laser ($t=250 \mu\text{s}$, $E=0.7 \text{ J cm}^{-2}$). The inset shows the forward current branch in logarithmic scale.

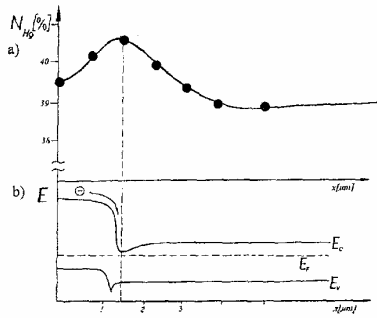


Fig.4. a) Distribution of Hg along the depth of the specimen (bN5) after annealing with three successive pulses with an energy density of $0.7 \text{ J}\cdot\text{cm}^{-2}$ and pulse lengths of $250\mu\text{s}$, obtained by X-ray microanalysis. b) The probably diagram for the energy bands for the heterojunction obtained.

The linear voltage-ampere characteristic (Fig. 3b) for HgCdTe after laser treatment is typical for heterojunctions.

The spatial distributions curves of the photo-signal in the photovoltaic mode $U(x,t)$ are presented in Fig.3a. Initially, samples were not photosensitive in the spectral range from 5 to $10 \mu\text{m}$ at 77 K. The photosignal decreased to zero when the probing laser beam was scanned beyond the irradiated area, as can be seen from Fig.3a. The photosignal observed may be only due to the presence of a potential barrier inside the sample.

Conclusions

The method using laser treatment for segregation of impurities or IMAs in solid phase $\text{Hg}_{0.8}\text{Cd}_{0.2}\text{Te}$ is presented. The model of thermodiffusion processes at laser annealing without melting is proposed. Computer simulation of these processes reveals the possibility of obtaining a sharp maximum of mercury concentration for chosen parameters of laser pulse. The result was experimentally verified with MCT specimens annealed by using a neodymium laser. X-ray analysis of the annealed samples has shown unexpected oscillations regularly repeated in each sample. Photoresponse and voltage-ampere characteristics show that the heterojunction is created in laser annealed HgCdTe. The heterojunction is photosensitive in the range $9\text{--}11 \mu\text{m}$.

References

1. G.G.Gromov, S.W.Seregin, S.V.Zuk, V.B.Ufimtsev, *Fiz. Khim. Obrabotki Mater.* **4**, 19 (1990).
2. A.Baidulaeva, B.K.Dauletmuratov, V.A.Gnatiuk, P.E.Mozol, *Phys. Stat. Sol. (b)* **122**, 243 (1990).
3. V.H.Strekalov, *Fiz. Tekh. Poluprov.* **20**, 361 (1986).
4. A.V.Dvurechenskii, V.G.Remesnic, N.Ch.Talipov, I.A.Riazantsev, *Fiz. Tekh. Poluprov.* **27**, 168 (1993).
5. P.E.Mozol, V.A.Gnatiuk, A.V.Sukach, A.I.Vlasenko, A.S.Kopishinskaja, V.I.Lukianenko, *Fiz. Tekh. Poluprov.* **27**, 1820 (1993).
6. A.A.Zaginei, B.K.Kotliarchuk, G.V.Pliatsko, V.G.Savitskii, *Neorg. Mater.* **25**, 1108 (1989).
7. C.N.Afonso, M.Alonso, J.L.H.Neira, A.D.Sequeira, M.F.da Silva, J.C.Soares, *J. Vac. Sci. Technol.* **A7**, 3256 (1989).
8. K.D.Tovstyuk, G.V.Pliatsko, V.B.Orletskij, S.G.Kijak, Ya.U.Bobitskij, *Ukr. Fiz. Zh.* **21**, 1918 (1976).
9. R.V.Luciv, V.G.Savitskij, G.V.Plyatsko, *Sov. Phys. Semicond.* **12**, 247 (1978).
10. S.Damquard, M.Oron, J.W.Petersen, *Phys. Stat. Sol. (a)* **59**, 63 (1980).
11. S.G.Kiyak, W.Krechun, A.A.Manenkov, *Fiz. Tekh. Poluprov.* **23**, 421 (1989).
12. V.P.Voronkov, G.A.Gurchenok, *Fiz. Tekh. Poluprov.*, **24**, 1831 (1990).
13. W.B.Fiks, *Przewodnictwo Jonowe w Metalach i Półprzewodnikach* (Warszawa, PWN, 1971).
14. R.Ciach, M.Faryna, M.Kuźma, M.Pociask, E.Shererii, *Thin Solid Films* **241**, 151 (1994).
15. M.Kuźma, M.Pociask, A.Wal, E.Shererii, J.Smela, *Modelling Simul. Mater. Sci. Eng.* **2**, 329 (1994).
16. D.Potter, *Computational Physics*, (John Wiley & Sons, London, New York, Sydney, Toronto 1973).
17. F.A.Zaitov, A.W.Gorshkov, G.M.Shaliapina, *Fiz. Tverd. Tela* **20**, 1601 (1978).

18. V.I.Ivanov-Omskii, N.N.Berchenko, A.I.Elizarov, *Phys. Stat. Sol.* **103**, 11 (1987).
19. J.Piotrowski, A.Rogalski, *Półprzewodnikowe Detektory Podczerwieni* (Warszawa, WNT, 1978).
20. R.Ciach, M.Faryna, M.Kuźma, M.Pociask, E.Sheregii, *Journal of Crystal Growth*, **161**, 234 (1996).
21. A.G.Khachaturian, *Theory of Phase Transitions and Structure of Solid Solution* (Moscow, 1974) [in Russian].
22. J.W.Cahn, *Acta Met.* **9**, 795 (1961).
23. J.W.Cahn, *Trans. AIME* **242**, 166 (1968).
24. E.Sheregii, M.Kuźma, C.Abeynayake, M.Pociask, *Can. J. Phys.* **73**, 174 (1995).

СТВОРЕННЯ ГЕТЕРОПЕРЕХОДІВ І ПЕРІОДИЧНИХ СТРУКТУР У ТВЕРДОМУ РОЗЧИНІ ЛАЗЕРНИМ ВІДПАЛОМ

М.М.Поцяск, Є.М.Шерегій, М.Кузьма

Інститут фізики, Педагогічний університет, Жешув, Польща
e-mail: pociask@atena.univ.rzeszow.pl

Представлено термодифузійну модель лазерного відпалу і розкладу матеріалу. Показано, що значну роль у цьому процесі відіграє фононний потік. Величина фононного потоку тісно пов'язана з областю матеріалу, де є значний градієнт температури, внаслідок чого атоми Hg збираються в області, що відповідає максимальному значенню градієнта температури. Показано, що процеси дифузії атомів при лазерному відпалі HgCdTe можуть викликати особливі умови розкладу твердого розчину. Експериментально реалізовано ідею можливого утворення *p-n*-гетеропереходу, показану в результаті комп'ютерного моделювання процесу транспорту маси при лазерній обробці HgCdTe. Зразки HgCdTe було опромінено без плавлення YAG:Nd-лазером. Наявність гетеропереходу недалеко від поверхні підтверджено фотовольтаїчними вимірюваннями та рентгенівським мікроаналізом, а також вольт-амперними характеристиками.